Archives of Biochemistry and Biophysics 496 (2010) 123–131

Contents lists available at ScienceDirect

Archives of Biochemistry and Biophysics

journal homepage: www.elsevier.com/locate/yabbi

Recombinant expression, purification, and characterization of ThmD, the oxidoreductase component of tetrahydrofuran monooxygenase ☆

Michelle Oppenheimer [a], Brad S. Pierce [b], Joshua A. Crawford [b], Keith Ray [a], Richard F. Helm [a], Pablo Sobrado [a,*]

[a] Department of Biochemistry, Virginia Tech., Blacksburg, VA 24061, USA
[b] Department of Chemistry and Biochemistry, University of Texas at Arlington, TX 76019, USA

ARTICLE INFO

Article history:
Received 22 December 2009
and in revised form 9 February 2010
Available online 14 February 2010

Keywords:
Tetrahydrofuran monooxygenase
Oxidoreductase
Flavoenzyme
Flavin-binding domain
Covalent flavin
Cytochrome *c* reductase
Iron–sulfur center

ABSTRACT

Tetrahydrofuran monooxygenase (Thm) catalyzes the NADH-and oxygen-dependent hydroxylation of tetrahydrofuran to 2-hydroxytetrahydrofuran. Thm is composed of a hydroxylase enzyme, a regulatory subunit, and an oxidoreductase named ThmD. ThmD was expressed in *Escherichia coli* as a fusion to maltose-binding protein (MBP) and isolated to homogeneity after removal of the MBP. Purified ThmD contains covalently bound FAD, [2Fe–2S] center, and was shown to use ferricyanide, cytochrome *c*, 2,6-dichloroindophenol, and to a lesser extent, oxygen as surrogate electron acceptors. ThmD displays 160-fold preference for NADH over NADPH and functions as a monomer. The flavin-binding domain of ThmD (ThmD-FD) was purified and characterized. ThmD-FD displayed similar activity as the full-length ThmD and showed a unique flavin spectrum with a major peak at 463 nm and a small peak at 396 nm. Computational modeling and mutagenesis analyses suggest a novel three-dimensional fold or covalent flavin attachment in ThmD.
Published by Elsevier Inc.

Introduction

Bacterial multicomponent monooxygenases (BMM)[1] are diiron-containing enzymes that hydroxylate a variety of hydrocarbons [1,2]. The diiron cluster ligands are provided by the side chains of residues that make up the sequence motif (D/E)EX_2-H(X)$\sim_{100}\sim EX_2$H(D/E)[3]. BMMs consist of, at least, an NADH oxidoreductase component, a hydroxylase component, which houses the diiron center, and a small protein regulatory component [2]. The BMM family has been divided into five groups based on component composition and operon organization [4]. Because these enzymes are capable of tuning the diiron center to perform C–H bond cleavage and hydroxylation in a variety of substrates, they are believed to have a potential application in bioremediation [4,5]. There is a plethora of work regarding the mechanism of oxygen activation and several intermediates have been directly observed by using transient kinetic approaches and spectroscopy [1,6–8]. Similarly, there are several structures of hydroxylases in the reduced and oxidized states and in the presence and absence of substrates [9–13]. More recently, structures of toluene 4-monooxygenase in complex with its regulatory protein have provided information about the mechanism of regulation in this group of enzymes. It was shown that binding of the regulatory protein causes a series of changes extending ~25 Å from the active site along several helices on the toluene 4-monooxygenase hydroxylase component, poising the enzyme for oxygen activation [14].

Tetrahydrofuran monooxygenase (Thm) is one of the two members of Group 5 BMM. Thm was identified from *Pseudonocardia* sp. strain K1, which is capable of growing aerobically on tetrahydrofuran as the sole carbon source [15]. The hydroxylase enzyme of Thm is composed of only α and β subunits, which in solution are predicted to form a heterotetramer, $(\alpha\beta)_2$. In all of the BMM enzymes studied to date, the hydroxylase is composed of a dimer of three polypeptide chains, $(\alpha\beta\gamma)_2$ [2,4]. Therefore, this novel member of the BMM family represents a "simplified" monooxygenase complex. The oxidoreductase component, ThmD, is composed of an NADH-and FAD-binding domain and a [2Fe–2S] domain. ThmD is responsible for transferring electrons from NADH to the diiron center via the FAD and the [2Fe–2S] center (Fig. 1). The amino acid sequence between ThmD and other oxidoreductases is moderately conserved (30–60%) and the cofactor-binding motifs for the various domains are strictly conserved (Fig. 2). However, ThmD is the only member of this family of enzymes that contains a covalently bound flavin cofactor. Here we present the cloning,

☆ Funded in part by a grant from ACS-Petroleum Research Fund to P.S.
* Corresponding author. Fax: +1 540 231 9070.
E-mail address: psobrado@vt.edu (P. Sobrado).
[1] *Abbreviations used*: BDR, benzoate 1,2-dioxygenase reductase; DCIP, 2,6-dichoroindophenol; DEAE, diethyl amino ethyl; ICP, inductively coupled plasma; IMAC, immobilized metal affinity chromatography; IPTG, isopropryl-β-thio galactopyranoside; MBP, maltose binding protein; MMOR, methane monoxygenase; PHR, phenol hydroxylase; T4MOF, toluene monooxygenase.

0003-9861/$ - see front matter Published by Elsevier Inc.
doi:10.1016/j.abb.2010.02.006

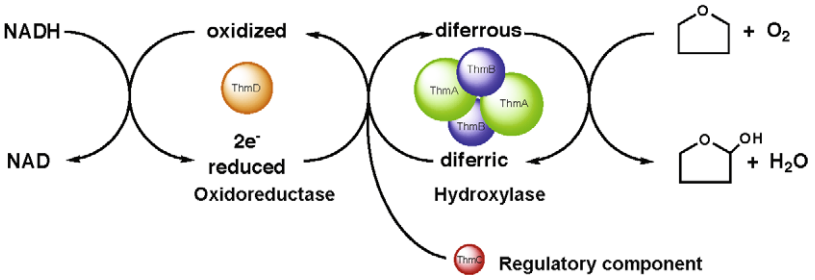

Fig. 1. Catalytic cycle of tetrahydrofuran monooxygenase. In the first step, reducing equivalents are transferred from NADH to the oxidoreductase, ThmD. ThmD reduces the diiron center housed in the ThmA subunit of the hydroxylase enzyme, ThmH. ThmH then reacts with molecular oxygen to hydroxylate tetrahydrofuran (THF). ThmH is predicted to be activated by the regulatory component, ThmC.

```
                1        10        20        30        40        50        60
ThmD  ....MGTFNVRFEPIGEEIECGEDETILDAAFRSGLNLVHGCREGRCSACKAFVLDEGWIYLKK.YSSFA
PHR   .....MSYQVTIEPVGMTIEVEEDQTILDAALRQGVWLPFACGHGTCGTCKVQVTDG.FYDVGE.ASPFA
TMOF  ......MFNIQSDDLLHHFEADSNDTLLSAALRAELVFPYECNSGGCGACKIELLEGEVSNLWP.DAPGL
MMOR  MQRVHTITAVTEDGESLRFECRSDEDVITAALRQNIFLMSSCREGGCATCKALCSEG.DYDLKG.CSVQA
BDR   .MSNHQVALQFEDGVTRFICIAQGETLSDAAYRQQINIPMDCREGECGTCRAFCESGNYDMPEDNYIEDA
                                                  *    *  *

                70        80        90       100       110       120       130
ThmD  LSDQEEEGGYTLLCRAVPESDVTIELLNYDPDHYRLEHAITDGVGQVVEVEALTHDIRRLELQIESPQG.
PHR   LMDIEREENKVLACCCKPESDMVIEAD.VDEDEDFLGYLVQDYQAKVLEIKQLSPTIKGVRLQIDRP...
TMOF  AAR.ELRKNRFLACQCKPLSDLKIKVINRAEG..RASHPPKRFSTRVVSKRFLSDEMFELRLEAEQK...
MMOR  LPPEEEEEGLVLLCRTYPKTDLEIELPYTHCRISFGEVG..SFEAEVVGLNWVSSNTVQFLLQKRPDECG
BDR   LTPEEAQQGYVLACQCRPTSDAVFQIQASSEVCKTKIHHFEGTLARVENLSDSTITFDIQLDDGQPD...
                *

                140       150       160       170       180       190       200
ThmD  ...FGFLPGQFVDIWIPGTEQRRSFSMANLPSD.GRLEFIIKQYPGGRFGALLDDGLAVGDPVKFTGPYG
PHR   ...MEFQAGQYINLQLPNIEGTRAFSIANPPSEEGIIELHIRQVLGGTATTYVHETLQAGDELQVSGPYG
TMOF  ...VVFSPGQYFMVDVP.ELGTRAYSAAN.PVDGNTLTLIVKAVPNGKVSCALAN..ETIETLQLDGPYG
MMOR  NRGVKFEPGQFMDLTIPGTDVSRSYSPANLPNPEGRLEFLIRVLPEGRFSDYLRNDARVGQVLSVKGPLG
BDR   ...IHFLAGQYVNVTLPGTTETRSYSFSSQPGN.RLTGFVVRNVPQGKMSEYLSVQAKAGDKMSFTGPFG
                R.YS                                    G..G..L.....G.....P.G

                210       220       230       240       250       260       270
ThmD  TCYLRDTGGSRSALLIAGGSGMAPILSLLRQMSDDGQGRTVSVFYGGRTRRDLFYTELVQSLGKRIEQFE
PHR   QFFVRKSD.EKDAIFIAGGSGLSSPQSMILDLLEQGDTRTIYLFQGARDVSELYNREVFETLVKDYPNFR
TMOF  LSVLKTAD.ETQSVFIAGGSGIAPMVSMVNTLIAQGYEKPITVFYGSRLEAEL...EAAETLFGWKENLK
MMOR  VFGLKERG.MAPRYFVAGGTGLAPVVSMVRQMQEWTAPNETRIYFGVNTEPELFYIDELKSLERSMRNLT
BDR   SFYLRDVK..RPVLMLAGGTGIAPFLSMLQVLEQKGSEHPVRLVFGVTQDCDLVALEQLDALQQKLPWFE
                M...GSGI.P

                280       290       300       310       320       330       340
ThmD  FIQVVSDEPDSDGDDVRYGFVHDAVDQWIETSGFRLDACDVYMAGPPPMVDAVNDVLTLRHQVEQNRIFV
PHR   YIPALNAPKTEDQWTGFTGFVHEAVADYFEN...KCSGHKAYLCGPPPMIDAAISTLMQSRLFEKD.IHT
TMOF  LINVSSSVVGNSEKKYPTGYVHEIIPEYMEG....LLGAEFYLCGPPQMINSVQKLLMIENKVPFEAIHF
MMOR  VKACVWHPSGD..WEGEQGSPIDALREDLES...SDANPDIYLCGPPGMIDAACELVRSR.GIPGEQVFF
BDR   YRTVVAHAESQHERKGYVTG..HIEYDWLNG.....GEVDVYLCGPVPMVEAVRSWLDTQGIQPANFLFE

                350       360
ThmD  DKFTSTGPEDSADSDSVSSL..
PHR   ERFLSAADGASNQARSALFRHI
TMOF  DRFF..................
MMOR  EKFLPSGAA.............
BDR   KFSAN.................
```

Fig. 2. Multiple sequence alignment of various oxidoreductase enzymes: tetrahydrofuran monooxygenase (ThmD), phenol hydroxylase reductase (PHR), toluene-4-monooxygenase (TMOF), methane monooxygenase (MMO), benzoate 1,2-dioxygenase reductase (BDR). Conserved residues are shown in the red box, and similar residues in red color. The four conserved cysteines that make up the [2Fe–2S] center are labeled with an asterisk (*). The predicted dinucleotide-binding regions; RxYS, GxxL(x)$_6$G(x)$_7$PxG, and M(x)$_3$GSGIxP are shown below the alignment [40]. Start of the Thm flavin domain is indicated by an arrow. Grey triangles indicate residues selected for mutagenesis studies.

expression, purification, and characterization of the full-length ThmD enzyme and its flavin domain (ThmD-FD) and computational and mutagenesis studies that suggest that the mode of flavin attachment in ThmD appears to be novel.

Materials and methods

Material

All buffers and media components were obtained from Fisher Scientific (Pittsburgh, PA). BL21TI^R chemical competent cells, NADH, NADPH, and cytochrome *c* (cyt *c*) were obtained from Sigma–Aldrich (St. Louis, MO). DNA primers were synthesized by Integrated DNA Technologies (Coralville, IA). Isopropyl β-thiogalactopyranoside (IPTG) was obtained from Gold biotechnology (St. Louis, MO) and DNA gel extraction and plasmid DNA purification kits were from Qiagen (Valencia, CA). *Escherichia coli* TOP-10 chemically competent cells were from Invitrogen (Carlsbad, CA). *Pme*I/*Sgf*I enzyme blend was from Promega (Madison, WI). Chromatographic columns were obtained from GE Healthcare.

Bioinformatics analysis

Amino acid sequence alignment was done using the Clustal W program included in the DNAstar program package (Madison, WI). Fig. 2 was created using the program Espript 2.2 (http://espript.ibcp.fr/ESPript/ESPript/). The program Pyre (http://www.sbg.bio.ic.ac.uk/phyre/) was used to create the threading-based three-dimensional model of ThmD [16].

Cloning the full-length ThmD

The gene coding for ThmD was amplified by polymerase chain reaction (PCR) directly from *Pseudonocardia* sp. strain K1 genomic DNA (generous gift of Prof. B. Theimer) using the ThmD (F) and ThmD (R) primers (Table 1). A single PCR product of ~1300 bp was observed on a 0.8% agarose gel, corresponding to the expected size of the ThmD gene (1355 bp). The DNA band was excised from the gel, purified, and digested with *Pme*I/*Sgf*I restriction enzyme blend at 37 °C for 40 min. The reaction was stopped by heat denaturation at 65 °C for 30 min. This sample was ligated into the pVP56 K plasmid, which was previously digested with *Pme*I and *Sgf*I using T4 ligase. This plasmid allows the expression of ThmD as a fusion to an 8xHis-maltose-binding protein (8xHis-MBP) and carries a kanamycin resistant marker. A ligation reaction was also performed with the pVP55A plasmid for the expression of ThmD as a fusion with an 8xHis tag. This plasmid carries an ampicillin resistant marker (both plasmids where obtained from the Center for Eukaryotic Structural Genomics, University of Wisconsin, Madison) [17]. Ligation reactions were transformed into chemically competent TOP-10 cells and plated in Luria–Bertani (LB) agar supplemented with the corresponding antibiotic and incubated overnight at 37 °C. Five colonies from each ligation reaction were used to inoculate five 10 mL LB cultures supplemented with the appropriate antibiotic and grown overnight at 37 °C. Plasmids were isolated using a Qiagen Kit and those plasmids containing the ThmD gene were identified by PCR using gene specific primers. The complete coding region was sequenced to ensure that no unwanted mutations were incorporated during the PCR reactions.

Engineering of ThmD-FD and ThmD-[2Fe–2S] domain

Amino acid sequence alignment of several members of the BMM oxidoreductase family was used to delineate the various domains in ThmD (Fig. 2). The [2Fe–2S]-binding domain corresponded to the first ~100 amino acids of the N-terminus. This region contains all four essential cysteine residues that bind the irons [18–20]. To clone this domain, the ThmD-[2Fe–2S] (R) and ThmD (F) primers were used in a PCR reaction using the wild-type ThmD gene as a template (Table 1). Primers ThmD-FD (F) and ThmD (R) were used to obtain the DNA fragment coding for residues 102–360, which correspond to the flavin and the NADH-binding domains. The truncated forms of ThmD were cloned into the pVP55A plasmid in frame with an N-terminus 8xHis tag as described above for the ThmD full-length protein.

Site-directed mutagenesis

Site-directed mutagenesis was performed using the QuikChange protocol (Stratagene, CA). Residues were selected for mutagenesis studies based of their proximity to the flavin cofactor in the model structure of ThmD (Fig. S1).

Expression of ThmD

Expression of ThmD fused to an 8xHis tag (in the pVP55A plasmid) was performed in LB medium supplemented with 200 μg mL^{-1} of ampicillin and incubated at 37 °C with agitation set at 250 rpm. Clones were transformed into BL21TI^R cells and grown on LB agar plates. After 24 h incubation, a single colony was used to inoculate a 50 mL LB starter culture and incubated overnight. Four cultures each of 1.5 L of LB media were inoculated with 10 mL of the overnight culture and incubated until the optical density measured at 600 nm (OD_{600}) reached a value of ~0.8, at which point protein expression was induced by addition of 0.5 mM IPTG. After 4 h induction, the cultures were harvested by centrifugation at 5000*g* for 20 min and the cell pellet stored at −80 °C. ThmD expressed well as a fusion to an N-terminal 8xHis tag; however, this protein was completely insoluble. After modifying the expression and purification procedures, we were unable to obtain soluble enzyme in this form. ThmD was obtained in a partially soluble form when expressed as a fusion to MBP using the pVP56 K plasmid. Throughout the expression of ThmD in pVP56 K, the LB media was supplemented with 50 μg mL^{-1} kanamycin with agitation set at 250 rpm. A single colony of BL21TI^R transformed with pVP56 K ThmD was used to inoculate a 50 mL LB culture. This culture was incubated at 37 °C. The next day, 6 culture flasks containing 1.5 L of LB supplemented with 0. 5 M NaCl were each inoculated with 7 mL of the overnight culture. These cultures were grown at 37 °C until the OD_{600} reached a value of ~0.6. The incu-

Table 1
Primers used for cloning ThmD and its truncated forms containing the flavin domain and [2Fe–2S] centers[a].

Primer	Restriction site	Amino acids	Sequence
ThmD (F)	*Sgf*I	1–360	5′-GGTTGCGATCGCATGGGAACCTTCAACGTAAGGTTCG-3′
ThmD (R)	*Pme*I	1–360	5′- AAAAGTTTAAACAAGCGACGATACAGAATCGG-3′
ThmD-FD (F)	*Sgf*I	102–360	5′-TTCGGCGATCGCCCATGCAATTACCGATGGAGTTGGCC-3′
ThmD-[2Fe–2S] (R)	*Pme*I	1–101	5′-AGCAGTTTAAACTGCATGCTCTAGCCGATAGTGGTCAGG-3′

[a] F and R are the forward and reverse primers, respectively.

bation temperature was increased to 47 °C for 30 min. After this heat shock period, protein expression was induced by addition of 300 μM IPTG and the media was supplemented with 150 mg ferric citrate, 150 mg ammonium ferric citrate, and 363 mg L-cysteine [21]. The cultures were incubated overnight at 10 °C. Cells were harvested by centrifugation at 5000*g* for 20 min and the cell pellet stored at −80 °C. This procedure regularly yielded 20 g of cell paste.

Expression of ThmD-FD and ThmD-[2Fe–2S] domain

ThmD-FD and ThmD-[2Fe–2S] domains were expressed using the plasmid pVP55A, which produced the recombinant protein as an N-terminal fusion to an 8xHis tag. Recombinant ThmD-[2Fe–2S] domain was found to be completely insoluble. Thus, no further experiments were performed with this truncated form of ThmD. For the ThmD-FD, a single colony of BL21TI^{R} containing the pVP55AThmD-FD plasmid was used to inoculate a 50 mL LB culture and incubated at 37 °C. The next day, 4 flasks, each containing 1.5 L of LB medium were inoculated with 10 mL of overnight culture. These cultures were incubated at 37 °C until the OD_{600} reached a value of 0.6. Protein expression was induced by addition of 0.5 mM IPTG. After 4 h of incubation at 37 °C, the cells were harvested by centrifugation at 5000*g* for 20 min. This protocol normally yielded ∼30 g of cell paste. All mutants of ThmD-FD were expressed following the same procedure as wild-type ThmD-FD.

Purification of ThmD

Cell pellets (∼20 g) were resuspended in 90 mL 25 mM HEPES, at pH 6.5, 420 μM tris(2-carboxyethyl)phosphine (TCEP), 0.75 mM phenylmethyl sulfonylfluoride (PMSF), 15 μg/mL DNase, 15 μg/mL RNase, and 15 μg/mL lysozyme, and stirred at 4 °C for 20 min. Cells were lysed by sonication for 5 min (5 s on, 10 s off). Insoluble fractions and unlysed cells were precipitated by centrifugation at 30,000*g* for 1 h at 4 °C. The resulting supernatant was loaded onto a diethyl amino ethyl (DEAE) column previously equilibrated in 25 mM HEPES at pH 6.5. After washing the column with 100 mL of 25 mM HEPES at pH 6.5 containing 140 mM NaCl, a 125 mL gradient of 140–400 mM NaCl was used to elute the MBP–ThmD fusion protein from the column. Fractions containing MBP–ThmD were identified by sodium dodecyl sulfate polyacrylamide gel electrophoresis (SDS–PAGE) and only those with the spectrum characteristic of a [2Fe–2S] cluster were pooled. Tobacco etch virus (Tev) protease was added (1:10) to liberate ThmD from MBP. The reaction was incubated at 4 °C overnight and the solution was centrifuged at 30,000*g* for 20 min to remove precipitated proteins before being loaded onto a nickel immobilized metal affinity chromatography (IMAC) column. Since both MBP and Tev proteins have an 8xHis tag these proteins remained bound, and the flow through containing free ThmD was collected. This sample was diluted 10-fold and loaded onto a second DEAE column. The column was washed with 50 mL of 25 mM HEPES, 150 mM NaCl, pH 7.5, followed by a 350 mL gradient from 150 to 400 mM NaCl in the same buffer. Fractions containing ThmD were identified by SDS–PAGE and by spectra analyses. Those fractions that were brown in color and showed spectra similar to Fig. 4 were pooled concentrated and loaded onto a S-200 Sephadex column previously equilibrated in 25 mM HEPES, 125 mM NaCl, pH 7.5. This step separated ThmD from some high molecular weight contaminants yielding more than 95% pure protein. The final sample was stored at −80 °C.

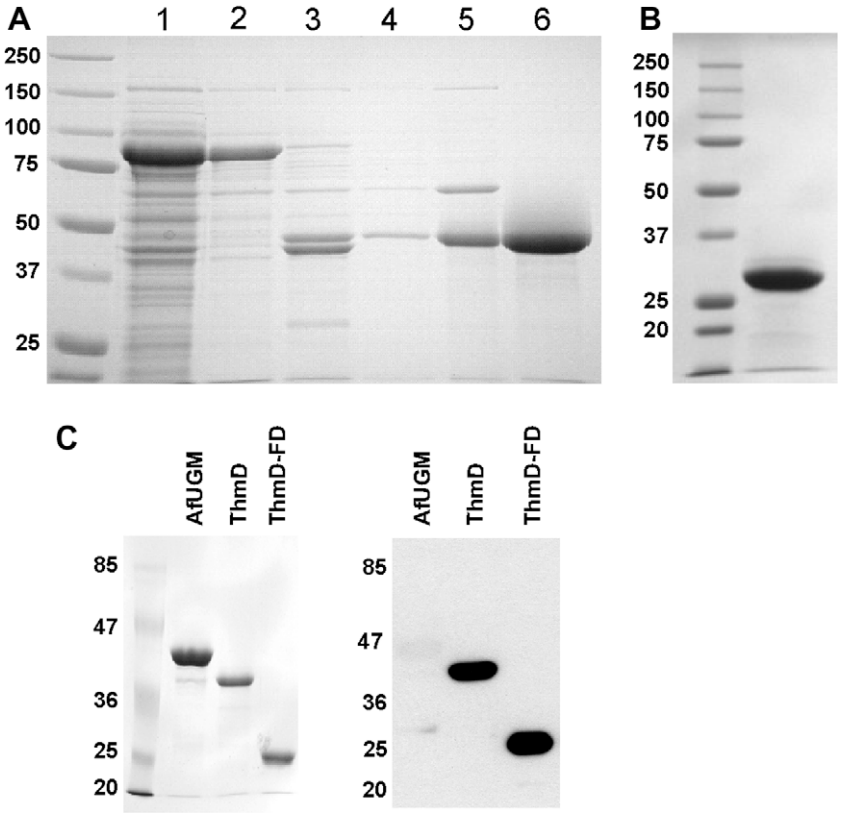

Fig. 3. (A) Coomassie stained SDS–PAGE analysis of ThmD from different steps of purification. Lane 1, lysate supernatant; lane 2, after DEAE chromatography at pH 6.5; lane 3, after treatment with Tev protease; lane 4, after nickel IMAC; lane 5, after second DEAE chromatography at pH 7.5; lane 6, after size exclusion chromatography. (B) Coomassie stained SDS–PAGE showing ThmD-FD after size exclusion chromatography. (C) Right panel shows the SDS–PAGE of the flavoenzyme UDP-galactopyranose mutase from *Aspergillus fumigatus* (AfUGM), ThmD, and Thm-FD. Left panel shows the Western-blot using anti-flavin antibody. Recombinant ThmD and ThmD-FD contain covalently attached flavin. The negative control, AfUGM, does not. The numbers on the left are the molecular weight standards.

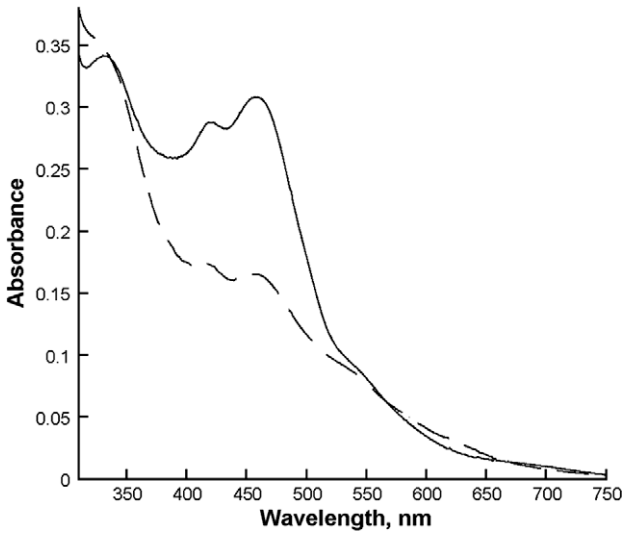

Fig. 4. Spectrum of the oxidized (solid lines) and reduced (broken lines) recombinant ThmD. The enzyme was reduced by addition of stoichiometric amounts of NADH.

Purification of ThmD-FD wild-type and mutant enzymes

Cell paste (~30 g) was resuspended in 150 mL 25 mM HEPES, 300 mM NaCl, 20 mM imidazole, 1 mM PMSF, and 25 μg/mL each of lysozyme, DNase, and RNase, at pH 7.5 and sonicated and centrifuged as described above for ThmD. Supernatant containing ThmFD was loaded onto a 5 mL nickel IMAC previously equilibrated with 25 mM HEPES, 300 mM NaCl, and 20 mM imidazole, at pH 7.5. The column was washed with the same buffer until the absorbance at 280 nm was near zero, at which point the bound yellow protein was eluted with buffer containing 25 mM HEPES, 300 mM imidazole, and 300 mM NaCl at pH 7.5. At this step, the ThmD-FD was ~90% pure. The 8xHis tag was removed by addition of Tev protease (at a 1:20 ratio) and incubating overnight at 4 °C. To separate the Tev and 8xHis peptide from ThmD-FD, the solution was concentrated and diluted 10-fold to decrease the amount of imidazole and loaded onto a nickel IMAC. ThmD-FD no longer had affinity for the IMAC column and the Tev and 8xHis peptide remained bound. The flow through, containing ThmD-FD, was collected and concentrated for a final purification step on Superdex S-75 size exclusion chromatography equilibrated with 25 mM HEPES, 125 mM NaCl, at pH 7.5. The final sample was more than 95% pure and was stored at −80 °C (Fig. 3B).

Determination of covalent flavin binding in recombinant ThmD

To determine if the flavin cofactor in the recombinant ThmD was covalently attached, we denatured the protein and precipitated the protein by centrifugation. Both ThmD full-length and ThmD-FD wild-type and mutant proteins were denatured either by heating the protein samples at 95 °C for 5 min or by adding 1% SDS or 10% trichloroacetic acid followed by centrifugation at 18,000*g* for 10 min. If the pellets remained yellow, it indicated that the flavin remained covalently attached. Western-blot using a flavin specific antibody (generous gift from Dr. Dale Edmonson) was also used to determine if the flavin was covalently attached to the various proteins.

Activity assay

The activity of ThmD was determined using cyt *c*, 2,6-dichoroindophenol (DCIP), ferricyanide, and oxygen as electron acceptors. Assays were done at 25 °C in 1 mL 25 mM HEPES, 125 mM NaCl at pH 7.5, and the activity was determined by measuring the change in absorbance at 550 nm for cyt *c*, 420 nm for ferricyanide, or 600 nm for DCIP. Rates were then calculated using the extinction coefficients of 21.1 cm^{-1} mM^{-1}, 1.04 mM^{-1} cm^{-1}, and 6.2 mM^{-1} cm^{-1} for cyt *c*, ferricyanide and DCIP, respectively. The reactivity with molecular oxygen was measured directly by determining the amount of oxygen consumed is air-saturated buffer using an oxygen monitoring system from Hansatech (Norfolk, England). Protein concentration was determined using Bradford reagent [22]. Assays with varying concentrations of NADH or NADPH were done with 100 μM cyt *c*. Assays with varying concentrations of cyt *c*, ferricyaninde, DCIP, and oxygen were done with 400 μM NADH. The software KaleidaGraph (Synergy Software, Reading, PA) was used to fit the data shown in Fig. 5. The steady-state parameters k_{cat} and K_M were determined by fitting of the initial velocity and substrate concentration data to the Michaelis–Menten (Eq. (1)). The apparent substrate inhibition constant for cyt *c* (K_{ai}) was determined by fitting the data to (Eq. (2)).

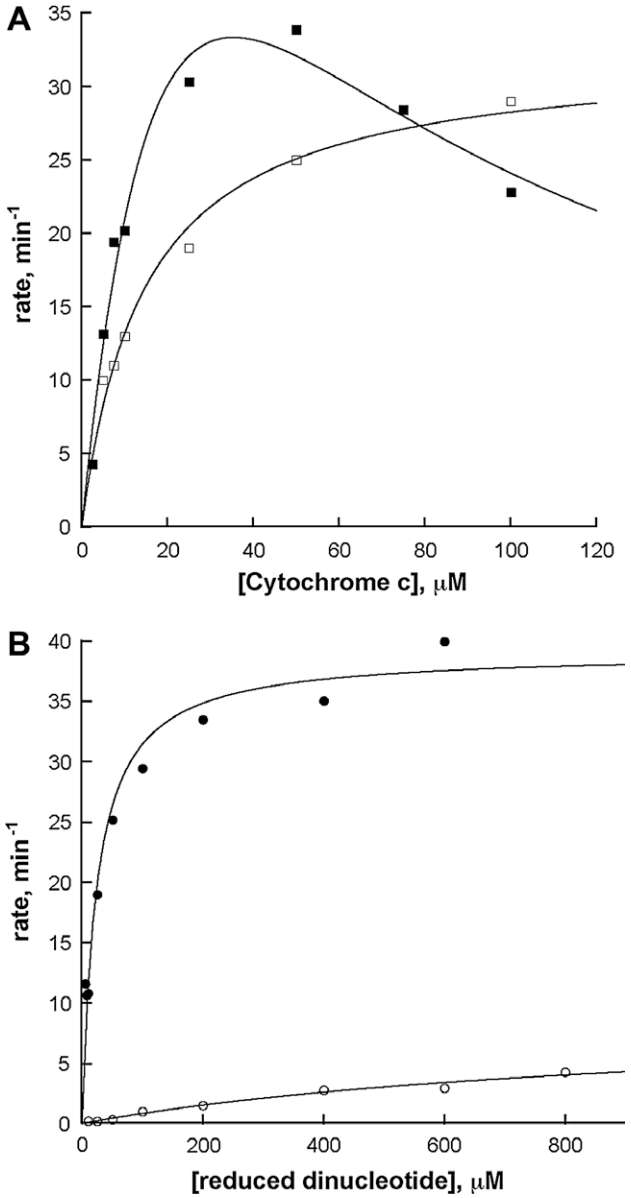

Fig. 5. (A) Steady-state kinetic analysis of ThmD (open square) and ThmD-FDT201A (close square) varying cytochrome *c* at saturating concentration of NADH (400 μM). (B) Kinetics of ThmD at various concentrations of NADH (solid circles) or NADPH (open circles).

$$v = \frac{k_{cat}A}{K_M + A} \quad (1)$$

$$v = \frac{k_{cat}A}{K_M + A + A^2/K_{Ai}} \quad (2)$$

Size exclusion chromatography

The solution molecular weight of ThmD was determined using a Superdex 200 10/300 GL column on an Äkta Prime system. Using a set of protein standards aproprotein (6.5 kDa), ribonuclease (13 kDa), carbonic anhydrase (29 kDa), ovalbumin (43 kDa), canolbumin (75 kDa), aldolase (158 kDa), and ferritin (440 kDa), we obtained a standard curve. Samples from four different preparations were loaded onto the column and the elution volumes calculated. The solution molecular weight was calculated using the method described by Andrews [23].

Metal analysis

ThmD samples were prepared at a final concentration of 3–4 μM (according to the Bradford assay) in 4 mL of 25 mM HEPES, 125 mM NaCl at pH 7.5. Samples were analyzed to determine iron content at the Virginia Tech Soil Testing Laboratory using inductively coupled plasma (ICP) emission spectrophotometer.

Electron paramagnetic resonance (EPR) spectroscopy

X-band (9 GHz) EPR spectra were recorded on a Bruker EMX Plus spectrometer equipped with a bimodal resonator (Bruker model 4116DM). Low-temperature measurements were made using an Oxford ESR900 cryostat and an Oxford ITC503S temperature controller. A modulation frequency of 100 kHz was used for all EPR spectra. All experimental data used for spin-quantitation were collected under nonsaturating conditions. EPR spectra were simulated and quantified using Spin Count (ver. 3.0.0), created by Professor M.P. Hendrich at Carnegie Mellon University. The spectral line width is dominated by *g*-strain. Therefore, simulations employ a Gaussian distribution in *g*-values to give the correct line width, specified as $\sigma g_{x,y,z}$. Least squares and deconvolution analysis of the spectra were combined to allow relevant parameters to vary while maintaining a sum of multiple species that best fit the experimental data. The simulations were generated with consideration of all intensity factors, both theoretical and experimental, to allow concentration determination of species. The only unknown factor relating the spin concentration to signal intensity was an instrumental factor that depended on the microwave detection system. However, this was determined by the spin standard, Cu(EDTA), prepared from a copper atomic absorption standard solution purchased from Sigma–Aldrich.

Results and discussion

Expression and purification of ThmD

Expression of ThmD in *E. coli* yields high amounts of recombinant protein; however, the ThmD fused to an N-terminus 8xHis tag was completely insoluble. Partially soluble protein was only obtained when ThmD was expressed as a fusion to MBP (Fig. 3A). MBP has been shown to increase the solubility of many proteins that are recombinantly expressed in *E. coli* [24–26]. Although expression of MBP–ThmD yielded partially soluble protein, only when the cells were subjected to heat-shock and the media was supplemented with iron and sulfur were we able to isolate ThmD with high levels of [2Fe–2S] cluster (Fig. 4). Heat-shock induces the expression of chaperone proteins that presumably help in the biogenesis of the [2Fe–2S] cluster in ThmD. To purify holo ThmD, a series of chromatographic steps were required. First the MBP–ThmD fusion was loaded onto a DEAE column at pH 6.5. Only fractions that were brown in color and showed a spectrum characteristic of a [2Fe–2S] contain protein were collected. A significant amount (>50%) of the fractions containing MBP–ThmD lacked the [2Fe–2S] center but were highly active since they contained the covalently bound FAD. After cleavage of the MBP, the sample was passed onto an IMAC to isolate the free ThmD from MBP, Tev and the 8xHis tag. A second DEAE column at pH 6.5 was necessary to separate holo ThmD from apo ThmD that only contained the flavin cofactor. A final size exclusion chromatographic step yielded homogeneous holo ThmD (Fig. 3 A). Expression of recombinant proteins that contain [Fe–S] centers in *E. coli* commonly suffer from low solubility and low cofactor incorporation [21,27]. This is particularly true within the family of bacterial multicomponent monooxygenases. Only recently reports of expression and purification of the oxidoreductase component of methane monooxygenase (MMOR), toluene monooxygenase (T4MOF), and phenol hydroxylase (PHR) have been published [19,27,28]. Most of the recombinant proteins produced were insoluble and a large portion of the soluble fraction did not contain the [2Fe–2S] cluster or flavin cofactor. For some enzymes such as TomoF, the oxidoreductase component of toluene/*o*-xylene monooxygenase, expression of soluble and active enzyme has not been accomplished. This enzyme was purified only after solubilization from inclusion bodies, refolding, and reconstitution of the cofactors [29]. The expression and purification procedures described here produced ~5–10 mg of pure ThmD from 20 g cell paste (Table 2). The combination of the expression of this enzyme with MBP, heat-shock expression method, and addition of iron and sulfur additives might be used to improve the solubility, stability, and cofactor incorporation of other oxidoreductases.

Expression and purification of ThmD domains

Previous work on the oxidoreductase component of methane monooxygenase has shown that the [2Fe–2S] and the flavin-binding domains can fold independently from each other and are functional. Furthermore, the expression and purification of MMOR components has led to the structural characterization of this enzyme using NMR and X-ray crystallography and has permitted the detailed characterization of the electron transfer processes using rapid-reaction kinetic analysis [19,30,31]. The amino acid sequence corresponding to the flavin- and NADH-binding domain was expressed and purified for the ThmD enzyme. The ThmD-FD protein was highly stable and contained covalently bound FAD.

Table 2
Purification of recombinant ThmD.

Step[a]	Total protein (mg)	Total activity (U)[b]	Activity recovered (%)	Specific activity (U/mg)	Fold purification
CL sup	3100	2290	100	0.73	1
DEAE1	200	116	5.0	0.58	0.78
DEAE2	10	9.5	8.2	0.95	1.25
SE	5.6	7	73	1.25	1.71

[a] CL sup: complete lysate supernatant, DEAE, diethylamino ethyl chromatography, SE, size exclusion chromatography.
[b] Unit is defined as 1 μmol of cytochrome *c* reduced/min at 25 °C.

Table 3
Steady-state kinetic parameters for ThmD and ThmD-FD[a].

Substrate	Kinetic parameters	ThmD	ThmD-FD
Cytochrome *c*[b]	k_{cat} (min^{-1})	42 ± 2	50 ± 5
	K_M (μM)	9 ± 2	18 ± 5
	k_{cat}/K_M (μM 1 min^{-1})	4.7 ± 1.0	2.8 ± 0.6
NADH[c]	k_{cat} (min^{-1})	39 ± 1	36 ± 2
	K_M (μM)	24 ± 4	15 ± 4
	k_{cat}/K_M (μM^{-1} min^{-1})	1.6 ± 0.3	2.4 ± 0.8
NADPH[c]	k_{cat} (min^{-1})	7.1 ± 1	13 ± 1
	K_M (μM)	692 ± 193	1092 ± 131
	k_{cat}/K_M (μM^{-1} min^{-1})	0.01 ± 0.0008	0.01 ± 0.002

[a] All the reactions were done in 1 mL 25 mM HEPES, pH 7.4 at 25 °C.
[b] Cyt *c* was varied while maintaining NADH saturation at 400 μM.
[c] These experiments were done with 100 μM cyt *c*.

Table 4
Steady-state kinetic parameters for ThmD and ThmD-FD with other electron acceptors[a].

Electron acceptor	Kinetic parameter	ThmD	ThmD-FD
DCIP	k_{cat} (min^{-1})	26 ± 1	35 ± 1
	K_M (μM)	7 ± 1	4.3 ± 0.7
	k_{cat}/K_M (μM^{-1} min^{-1})	3.7 ± 0.5	8 ± 1
FeCN	k_{cat} (min^{-1})	490 ± 30	600 ± 40
	K_M (μM)	70 ± 20	120 ± 30
	k_{cat}/K_M (μM^{-1} min^{-1})	7 ± 1	5 ± 0.9
Oxygen[b]	$_{app}k_{cat}$ (min^{-1})	10 ± 2	1.6 ± 0.1

[a] These reactions were done in 25 mM HEPES and 125 mM NaCl, pH 7.5, at 25 °C, containing 400 μM NADH.
[b] In air-saturated buffer.

In contrast, the ThmD-[2Fe–2S] domain was not soluble in *E. coli*. This is surprising since domains within the oxidoreductases have been well characterized. This represents another difference between ThmD and the other oxidoreductases.

Enzyme activity

The activity of ThmD in the Thm complex could not be assessed due to of the absence of recombinant monooxygenase component. Instead, we measured the activity of the recombinant ThmD enzyme and its flavin domain variants using cyt *c* as an artificial electron acceptor. A k_{cat} value of 42 min^{-1}, K_M of 9 ± 2 μM and a k_{cat}/K_M value of 4.7 ± 1.0 μM^{-1} min^{-1} were determined for ThmD with cyt *c* as the substrate (Table 3). There are no published data of the kinetic parameters with cyt *c* for the native ThmD enzyme purified from *Pseudonocardia* sp. strain K1, however, the a specific activity of 1.6 U/mg was reported for the native ThmD, this value is very close to the specific activity determined here for recombinant ThmD [33]. We can compare the activity of ThmD to the reported activity of phenol hydroxylase reductase with cyt *c* as substrate. For this enzyme a K_M value of 1.6 μM was calculated. This value is similar to that of ThmD. In contrast, a k_{cat} value of 4020 min^{-1} was reported, which is ~100-fold higher than for ThmD [28]. The activity of the ThmD-FD was also determined with cyt *c* (Table 3). A less than 2-fold decrease in the k_{cat}/K_M for this substrate was observed for the ThmD-FD as compared to ThmD. This change originated from a 2-fold increase in the K_M value for cyt *c* in ThmD-FD, suggesting that cyt c binds better to ThmD when the [2Fe–2S] domain is present.

For ThmD, a K_M value for NADH of 24 ± 4 μM was calculated which is similar to the K_M values reported for phenol hydroxylase reductase (36 μM) and benzoate 1,2-dioxygenase reductase (29 μM)[28,34]. ThmD displays reduced dinucleotide selectivity for NADH, as indicated by a 160-fold higher catalytic efficiency for NADH as compared to NADPH (Table 3 and Fig. 5). The activity of ThmD-FD with NADH is almost unchanged. With NADPH both k_{cat} and K_M increase by less than 2-fold, resulting in no change in the catalytic efficiency (Table 3).

The kinetic parameters with DCIP, ferricyanide, and molecular oxygen were also determined. With DCIP, ThmD and ThmD-FD have k_{cat} values around 30 min^{-1}, similar to the values with cyt *c*. With ferricyanide ThmD and ThmD-FD display higher k_{cat} values as compared to DCIP and cyt *c* (Table 4), however, the K_M value is more than 15-fold higher resulting in a k_{cat}/K_M value of ~6 μM^{-1} min^{-1}, which is very similar to the values with DCIP and cyt *c*. The k_{cat} values of phenol hydroxylase reductase with DCIP and ferricyanide as substrate are 780 and 1920 min^{-1}, respectively [28]. The lower activity of ThmD with cyt *c*, ferricyanide and DCIP as compared to phenol hydroxylase reductase might be explained by the differences in the amino acid sequences between the two enzymes, which are only 34% identical. Furthermore, the redox potential of the FAD in ThmD might be modulated by its covalent attachment in such a way that it is not optimal for reaction with cyt *c*.

UV–visible spectroscopy

The UV/vis-spectra of the oxidized ThmD shows absorbance maxima at 457, 419, and 330 nm, consistent with other known NADH oxidoreductases (Fig. 4) [19,21,27]. ThmD-FD shows significant differences in the spectrum of the bound flavin. There is a shift in the λ_{max} to 463 and only a small absorbance peak is observed at 396 nm. Spectra of oxidized flavins normally have two major absorbance peaks around 350 nm and 450 nm [19,27]. In ThmD-FD, the 350 nm peak is almost absent (Fig. 6). This difference in the spectra of the flavin might originate from a novel covalent attachment of the flavin or to different active-site architecture in ThmD as compared to other known oxidoreductases.

EPR spectroscopy

As isolated, no appreciable EPR signals were observed in samples of ThmD. The lack of an isotropic signal at $g = 4.3$ indicates the absence of adventitiously bound ferric iron. However, as shown in Fig. 7 (solid line), treatment with excess sodium dithionite and methyl viologen followed by anaerobic gel filtration re-

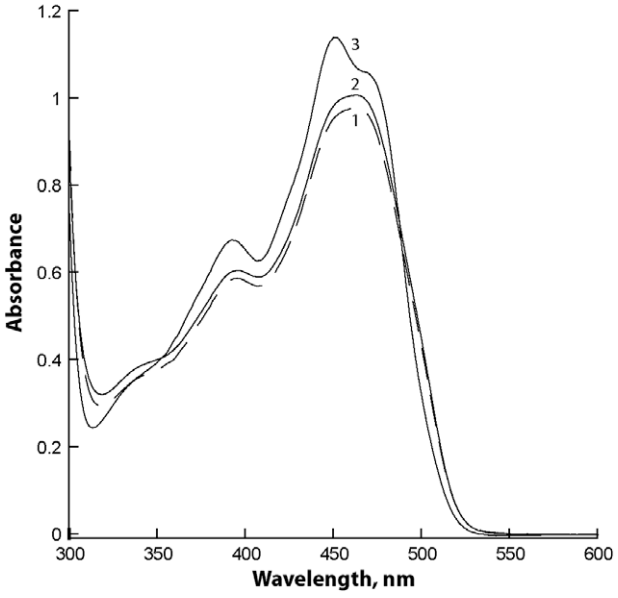

Fig. 6. Spectra of ThmD-FD (1) and the mutant variants T201A (2) and C202A (3). The spectrum of the Y199A mutant was identical to Thm-FD (not shown).

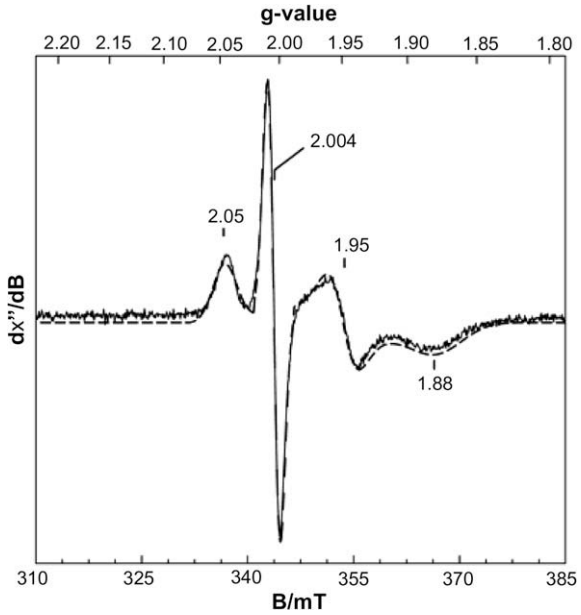

Fig. 7. X-band EPR spectrum of reduced ThmD (solid line). The ThmD sample was reduced with excess sodium dithionite in the presence of methyl viologen and then desalted anaerobically in a glove box to remove excess reductant. The resulting anaerobic protein concentration was ~40 μM. Instrumental parameters: microwave frequency, 9.64 GHz; microwave power, 20 μW; modulation amplitude, 9 mT; temperature, 10 K. Simulation parameters: spectrum A; $S = 1/2$; $g_{x,y,z} = 2.00$; $\mu_B = 0.9$ mT. Spectrum B; $S = 1/2$; $g_{x,y,z} = 2.047, 1.95, 1.875$; $\mu g_{x,y,z} = 0.009, 0.009, 0.018$; $\mu_B = 0.9$ mT. A quantitative component sum simulation (dashed line) for the spectra associated with species A and B was utilized to generate the simulation for this Figure. Using this technique, the respective concentration for each species was determined by least-squares analysis to be 2 and 34 μM, respectively.

sulted in the formation of two spectroscopically distinct $S = 1/2$ species termed A and B. The individual contribution of each was determined by quantitative simulation (dashed line) and least squares fitting. Species A exhibits an isotropic g-value ($g_{iso} = 2.00$) and inhomogeneous saturation with a half-saturation power ($P^{1/2}$) of 10 μW. Spin quantitation of A under nonsaturating conditions indicates < 2 μM, which represents 5% of the total protein concentration. Given that both dithionite and methyl viologen were removed by gel-filtration, species A can likely be attributed to the protein-bound neutral FADH-semiquinone radical. Both the saturation behavior at this temperature and the isotropic *g*-value are consistent with this assignment.

Species B exhibits rhombic EPR spectra with *g*-values of 2.05, 1.95, and 1.87. The observed *g*-anisotropy, and the fact that the average *g*-value ($g_{ave=}$1.96) is less than the free electron *g*-value ($g_e = 2.0023$) is diagnostic of an antiferromagnetically spin-coupled $Fe^{II}Fe^{III}$-cluster. When taken together with the saturation behavior ($P^{1/2} = 0.22$ mW) of species B at 10 K, the observed *g*-values clearly identify the presence of an intact $[2Fe–2S]^{1+}$ cluster [32]. A concentration of 34 ± 5 μM was determined for the [2Fe–2S] was determined for the $[2Fe–2S]^{1+}$ cluster by quantitative simulation under non-saturation conditions. This represents approximately 1.7 Fe atoms per protein.

Molecular weight determination

Purified recombinant ThmD migration on an SDS–PAGE gives an apparent molecular mass of ~40,000 Da. This value closely matches the predicted molecular weight that was calculated based on the amino acid sequence (39,845 Da). The molecular weight in solution was determined by size exclusion chromatography analysis and was calculated to be 52,000 ± 9000 Da, indicating that in solution the protein is present as a monomer, which is consistent with the other oxidoreductases.

Cofactor incorporation

Expression of 8xHis-ThmD resulted in insoluble protein. Only when the enzyme was expressed as a fusion to MBP did approximately 50% of the total recombinant enzyme remain in the soluble form. Metal analysis by ICP, indicated that isolated ThmD contains 1.7 ± 0.3 irons per subunit of enzyme. This was supported by quantitative EPR determination of total iron content in ThmD. Similarly, determination of the flavin content indicated stoichiometric amounts of FAD. The protein engineering and expression procedures described here might be used to improve the solubility and cofactor incorporation in other members of the oxidoreductase family of enzymes.

Site of covalent flavin attachment

ThmD is the only member among the oxidoreductase components from the BMM family that has been shown to contain a covalently bound flavin cofactor. Covalently bound flavins are found in only ~10% of all flavin-containing proteins, and they are bound to the side chains of histidine, tyrosine, or cysteine. The site of attachment to the flavin has mainly been observed at the C6 and Cα8-methyl group of the isoalloxazine ring. Only recently was a covalent attachment between the terminal phosphate of FMN in Na-translocating NADH-quinone reductase and a threonine residue been reported [35]. We analyzed the trypsin digest of ThmD using MALDI-TOF and LC-MS and were unable to conclusively identify a peptide containing a covalently bound flavin. Furthermore, we analyzed peptides resulting from the trypsin digest of ThmD-FD but were unable to identify the site of covalent attachment (not shown). To help us identify the site of flavin binding in ThmD, we created a three-dimensional model by threading the amino acid sequence of ThmD onto the structure of benzoate 1,2-dioxygenase from *Acinetobacter sp*. strain ADP1 (Fig. S1)[36]. This enzyme is 30% identical to ThmD. We also modeled the FAD cofactor to identify residues that are predicted to be in close proximity to the C6α- and C8α-methyl positions of the flavin. This analysis led us to mutate T201 and C202, because they are close to the C8α-methyl, and are not strictly conserved (Fig. 2). Mutagenesis of this residue to alanine produced soluble proteins that contained bound flavin. The spectra of the flavin in ThmD-FDT201A was identical to the ThmD-FD while the spectra of ThmD-FDC202A was different, suggesting that the protein microenvironment around the flavin had been changed (Fig. 6). Using heat, chemical, and acid denaturation, and western blot, it was determined that the flavin remained covalently attached to these mutants. Thus, T201 and C202 are not involved in covalent flavin attachment in ThmD. Steady-state kinetic analysis indicated that the mutant enzymes were able to utilize NADH with efficiencies similar to the wild-type enzyme (Table 5). Surprisingly, analysis of the activity with cyt *c* indicates that replacement of T201 and C201 with alanine induces substrate inhibition. However, the kinetic parameters were similar to wild-type ThmD-FD (Fig. 5 and Table 5). Close examination of the model structure showed that Y199 is in close proximity to the Cα8-methyl group of the flavin. Thus, this amino acid was also mutated to phenylalanine. Protein denaturation, spectrum and kinetic parameters with NADH showed that this residue is also not involved in flavin attachment or catalysis (Table 5).

We also searched for cysteines, tyrosines, threonines, or histidines that might be close to the C6α-methyl position, but none were found. The fact that the three-dimensional model of ThmD does not allow the identification of amino acids involved in flavinylation suggests that the three-dimensional fold of ThmD

Table 5
Steady-state kinetic parameters for ThmD-FD mutant enzymes[a].

Substrate	Kinetic parameters	Y199F	T201A	C202A
Cytochrome *c*[b]	k_{cat} (min^{-1})	51 ± 14	94 ± 38	106 ± 68
	K_M (μM)	15 ± 6	32 ± 7	44 ± 35
	k_{cat}/K ($\mu M^{-1}min^{-1}$)	3.4 ± 0.6	3.2 ± 0.6	3.1 ± 0.9
	K_i (μM)	104 ± 65	38 ± 23	25 ± 22
NADH[c]	k_{cat} (min^{-1})	31 ± 2	32 ± 1	29 ± 1
	K_M (μM)	9 ± 2	10 ± 2	4 ± 1
	k_{cat}/K_M ($\mu M^{-1}min^{-1}$)	3.6 ± 0.9	3.2 ± 0.6	6 ± 1

[a] All the reactions were done in 1 mL 25 mM HEPES, pH 7.4 at 25 °C.
[b] Cyt *c* was varied while maintaining NADH saturation at 400 μM.
[c] These experiments were done at 50 μM cyt *c* to prevent substrate inhibition.

might be different than other members of the oxidoreductase family of enzymes. It might also be possible that the site of covalent attachment is novel or perhaps there is a bi-covalent attachment of the FAD in ThmD. Recently, attachment of FAD cofactors at positions C6- and C8-alpha have been reported for the berberine bridge and chito-oligosaccharide oxidase enzymes [37,38]. Ultimately, the three-dimensional structure of ThmD or Thm-FD will provide clear evidence of the mode of covalent flavin attachment in this novel enzyme. Our protein expression and purification efforts will allow for the screening of conditions for crystallization of ThmD and this work is currently in progress.

Conclusions

Thm is a recently identified member of the BMM family of enzymes and the enzymes in this enzyme complex are different from other well-characterized systems such as methane monooxygenase and toluene 4-monooxygenase [14,39]. In the Thm operon, ThmA and ThmB, code for the hydroxylase component. These proteins are homologous to the α and β subunits of all other BMO hydroxylases, however, Thm does not contain a γ subunit like the other proteins. The oxidoreductase component in Thm also differs from all other BMOs. Among the members of the BMO oxidoreductases, ThmD is the only enzyme with a covalently bound flavin. In this work, we presented the cloning, expression, and purification of the recombinant form of ThmD. We showed that by expressing this enzyme as a fusion to MBP and in the presence of extra iron and sulfur in the growth medium, a soluble holo enzyme could be isolated. Heat-shock of the *E. coli* cells was also necessary, which suggests that chaperones might be necessary for the proper folding of recombinant ThmD. The resulting enzyme contained full cofactor incorporation, was active, and very stable. The flavin-binding domain containing covalently bound flavin was also cloned and isolated. This domain retained wild-type ThmD NADH oxidase and cyt *c* reductase activities. Modeling studies combined with site-directed mutagenesis failed to identify the site of covalent flavin attachment in ThmD-FD suggesting that the three-dimensional structure or the nature of the residue(s) involved in covalent attachment might be novel. This hypothesis is supported by the very peculiar flavin spectrum observed in the ThmD-FD enzyme. The work presented here sets the stage for future *in vitro* studies of the role of covalent flavin attachment in this unique enzyme by rapid kinetic analysis and X-ray structural determination.

Acknowledgments

The authors thank Dr. Dale Edmonson (Emory University, Atlanta, GA) for providing the anti-flavin antibody and Dr. Barbara Theimer (Martin-Luther-Universität Halle, Germany) for providing the *Pseudonocardia sp.* strain K1 genomic DNA. The authors also thanks Dr. M.P. Hendrich (Carnegie Mellon University) for providing the EPR analysis and simulation software (Spin Count) and the UTA Center for Nanostructured Materials (http://www.uta.edu/cos/cnm/) for the use of EPR instrumentation.

Appendix A. Supplementary data

Supplementary data associated with this article can be found, in the online version, at doi:10.1016/j.abb.2010.02.006.

References

[1] B.J. Wallar, J.D. Lipscomb, Chem. Rev. 96 (1996) 2625–2658.
[2] J.G. Leahy, P.J. Batchelor, S.M. Morcomb, FEMS Microbiol. Rev. 27 (2003) 449–479.
[3] B.G. Fox, J. Shanklin, J. Ai, T.M. Loehr, J. Sanders-Loehr, Biochemistry 33 (1994) 12776–12786.
[4] E. Notomista, A. Lahm, A. Di Donato, A. Tramontano, J. Mol. Evol. 56 (2003) 435–445.
[5] M.H. Sazinsky, J. Bard, J. Biol. Chem. 279 (2004) 30600–30610.
[6] E.Y. Tshuva, D. Lee, W. Bu, S.J. Lippard, J. Am. Chem. Soc. 124 (2002) 2416–2417.
[7] V. Guallar, B.F. Gherman, W.H. Miller, S.J. Lippard, R.A. Friesner, J. Am. Chem. Soc. 124 (2002) 3377–3384.
[8] J.A. Broadwater, C. Achim, E. Munck, B.G. Fox, Biochemistry 38 (1999) 12197–12204.
[9] A.C. Rosenzweig, P. Nordlund, P.M. Takahara, C.A. Frederick, S.J. Lippard, Chem. Biol. 2 (1995) 409–418.
[10] L.J. Murray, S.J. Lippard, Acc. Chem. Res. 40 (2007) 466–474.
[11] M.H. Sazinsky, P.W. Dunten, M.S. McCormick, A. Didonato, S.J. Lippard, Biochemistry 45 (2006) 15392–15404.
[12] L.J. Bailey, B.G. Fox, Biochemistry 48 (2009) 8932–8939.
[13] N.L. Elsen, L.J. Bailey, A.D. Hauser, B.G. Fox, Biochemistry 48 (2009) 3838–3846.
[14] L.J. Bailey, J.G. McCoy, G.N. Phillips Jr., Proc. Natl. Acad. Sci. USA 105 (2008) 19194–19198.
[15] B. Thiemer, J.R. Andreesen, T. Schrader, Arch. Microbiol. 179 (2003) 266–277.
[16] L. Kelly, M.J.E. Sternberg, Nat. Protoc. 4 (2009) 363–371.
[17] P.G. Blommel, P.A. Martin, K.D. Seder, R.L. Wrobel, B.G. Fox, Methods Mol. Biol. 498 (2009) 55–73.
[18] J. Muller, A.A. Lugovskoy, G. Wagner, S.J. Lippard, Biochemistry 41 (2002) 42–51.
[19] J.L. Blazyk, S.J. Lippard, Biochemistry 41 (2002) 15780–15794.
[20] J.L. Blazyk, S.J. Lippard, J. Biol. Chem. 279 (2004) 5630–5640.
[21] S. Jaganaman, A. Pinto, M. Tarasev, D.P. Ballou, Protein Expression Purif. 52 (2007) 273–279.
[22] M.M. Bradford, Anal. Biochem. 72 (1976) 248–254.
[23] P. Andrews, Biochem. J. 91 (1964) 222–233.
[24] P. Sobrado, M.A. Goren, D. James, C.K. Amundson, B.G. Fox, Protein Expr. Purif. 58 (2008) 229–241.
[25] W.B. Jeon, D.J. Aceti, C.A. Bingman, F.C. Vojtik, A.C. Olson, J.M. Ellefson, J.E. McCombs, H.K. Sreenath, P.G. Blommel, K.D. Seder, B.T. Burns, H.V. Geetha, A.C. Harms, G. Sabat, M.R. Sussman, B.G. Fox, G.N. Phillips Jr., J. Struct. Func. Genomics 6 (2005) 143–147.
[26] B.P. Austin, S. Nallamsetty, D.S. Waugh, N.J 498 (2009) 157–172.
[27] L.J. Bailey, N.L. Elsen, B.S. Pierce, B.G. Fox, Protein Expr. Purif. 57 (2008) 9–16.
[28] E. Pessione, S. Divari, E. Griva, M. Cavaletto, G.L. Rossi, G. Gilardi, C. Giunta, FEBS 265 (1999) 549–555.
[29] V. Cafaro, R. Scognamiglio, A. Viggiani, V. Izzo, I. Passaro, E. Notomista, F.D. Piaz, A. Amoresano, A. Casbarra, P. Pucci, A. Di Donato, FEBS 269 (2002) 5689–5699.
[30] L.L. Chatwood, J. Muller, J.D. Gross, G. Wagner, S.J. Lippard, Biochemistry 43 (2004) 11983–11991.
[31] D.A. Kopp, G.T. Gassner, J.L. Blazyk, S.J. Lippard, Biochemistry 40 (2001) 14932–14941.
[32] S.J.A.B. Lippard, J.M. Berg, Principles of Bioinorganic Chemistry, University Science Books, 1994.
[33] B. Thiemer, J.R. Andreesen, T. Schrader, FEBS 268 (2001) 3774–3782.
[34] M. Yamaguchi, H. Fujisawa, J. Biol. Chem. 253 (1978) 8848–8853.
[35] M. Hayashi, Y. Nakayama, M. Yasui, M. Maeda, K. Furuishi, T. Unemoto, FEBS Lett. 488 (2001) 5–8.
[36] G.T. Gassner, M.L. Ludwig, D.L. Gatti, C.C. Correll, D.P. Ballou, FASEB J. 9 (1995) 1411–1418.
[37] A. Winkler, F. Hartner, T.M. Kutchan, A. Glieder, P. Macheroux, J. Biol. Chem. 281 (2006) 21276–21285.
[38] C.H. Huang, W.L. Lai, M.H. Lee, C.J. Chen, A. Vasella, Y.C. Tsai, S.H. Liaw, J. Biol. Chem. 280 (2005) 38831–38838.
[39] M. Merkx, D.A. Kopp, M.H. Sazinsky, J.L. Blazyk, J. Muller, S.J. Lippard, Angew. Chem. Int. Ed. Engl. 40 (2001) 2782–2807.
[40] O. Dym, D. Eisenberg, Protein Sci. 10 (2001) 1712–1728.